Heliyon 10 (2024) e28954

Contents lists available at ScienceDirect

Heliyon

journal homepage: www.cell.com/heliyon

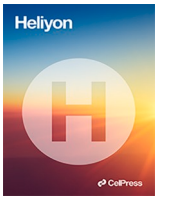

Research article

Baicalein improves renal interstitial fibrosis by inhibiting the ferroptosis *in vivo* and *in vitro*

Guo-qiang Liang [a,b,1], Wei Mu [d,1], Chun-bo Jiang [a,c,*]

[a] *Suzhou TCM Hospital Affiliated to Nanjing University of Chinese Medicine, Suzhou, China*
[b] *Suzhou Academy of Wumen Chinese Medicine, Suzhou, China*
[c] *Department of Nephrology, Suzhou Hospital of Traditional Chinese Medicine, Suzhou, China*
[d] *Department of Pharmacy and Clinical Pharmacy, Precision Medicine Center, 904th Hospital of PLA, Wuxi, China*

A R T I C L E I N F O

Keywords:
Baicalein
Renal interstitial fibrosis
Ferroptosis
TGF-β
GPX4

A B S T R A C T

Evidence indicates that Baicalein can ameliorate renal interstitial fibrosis by inducing myofibroblast apoptosis and inhibit the RLS3-induced ferroptosis in melanocytes. However, the relationship between renal interstitial fibrosis and anti-ferroptosis affected by Baicalein remains unclear. In our study, the anti-fibrosis and anti-ferroptosis effects of Baicalein were assessed in a rat model induced by the UUO method *in vivo*, and the effects of Baicalein on Erastin-induced ferroptosis of renal MPC-5 cells were examined by Western blot of fibrosis-related and ferroptosis-related proteins *in vitro*. In the UUO-induced rat model, Baicalein decreased kidney weight loss, improved renal function assessed the biomarks of urinary albumin excretion, serum creatine, and BUN levels, and reduced renal tubular injury. Furthermore, Baicalein inhibited renal ferroptosis by reducing ROS and MDA levels and increasing SOD and GSH levels in the UUO rat model. In addition, Baicalein potently reduced the expression of fibrosis-related proteins such as TGF-β1, a-SMA, and Smad-2 to prevent renal interstitial fibrosis, and increased the expression of ferroptosis-related proteins such as SLC7A11, GPX4, and FTH to inhibit ferroptosis both *in vitro* and *in vivo*. Taken together, Baicalein exerts anti-fibrosis activity by reducing the ferroptosis response on the UUO-induced rat model and renal MPC5 cells. Therefore, Baicalein, as a novel therapeutic method on kidney diseases with strong activity in suppressing ferroptosis, could be a potential alternative treatment for renal interstitial fibrosis.

1. Introduction

Renal interstitial fibrosis (RIF) is the excessive deposition of extra-cellular matrix (ECM) components in the renal interstitium caused by a variety of reasons such as trauma, inflammation, and blood circulation disorders. RIF often occurs in the glomerular podocytes that play an important role in glomerular basement membrane (GBM) remodeling, and interdigitating foot process with filtration slits in and between. Glomerular podocyte injury results in loss of foot process fusion and retraction, shrinkage of the cell body, formation of the pseudocyst, and reduced anionic charge, all of which led to the detachment of podocytes from GBM, the damage of fissure membrane, the high filtration of proteins, and kidney shrinking eventually [1].

* Corresponding author. Department of Nephrology, Suzhou Hospital of Traditional Chinese Medicine. NO. 899 Wuzhong West Road, Suzhou, 215000, China.
E-mail address: fsyy00569@njucm.edu.cn (C.-b. Jiang).
[1] The author had the same contribution to this work.

https://doi.org/10.1016/j.heliyon.2024.e28954
Received 21 November 2023; Received in revised form 19 March 2024; Accepted 27 March 2024
Available online 2 April 2024

Ferroptosis, an iron-dependent phospholipid peroxidation and high reactive oxidative stress (ROS), exists in many diseases occurring in the heart, brain, liver, kidney and so on. Accumulation of ROS derived from abnormal iron metabolism in kidney disease led to oxidative damage in renal cell membranes until it affected renal cell integrity and survival [2]. Recent studies demonstrated that ferroptosis played an important role in ischemia/reperfusion-induced acute kidney injury (AKI) [3]. Thus, from previous studies, we concluded that ferroptosis was involved in many kidney diseases frequently. However, there is little report about ferroptosis on the disease of RIF.

Baicalein, a type of polyphenolic flavonoid, is extracted from the roots of *Scutellaria baicalensis Georgi,* with effects of anti-tumor, anti-fibrogenesis, anti-inflammatory, cardiovascular protective effects and so on [4]. As a potential antioxidant, Baicalein has been used against fibrosis diseases in the kidney, myocardium, lung, and liver [5]. There are a lot of reports on the anti-ferroptosis effect of Baicalein such as inhibiting RLS3-induced ferroptosis in melanocytes and exerting neuroprotective effects in $FeCl_3$-induced post-traumatic epileptic seizures [6,7]. However, whether Baicalein has an anti-ferroptosis effect on RIF remains unclear. In this study, we elucidated the molecular mechanism of Baicalein on anti-ferroptosis and inferred that Baicalein had a potential effect on RIF treatment.

2. Materials and methods

2.1. Animals and housing

Sprague Dawley (SD) rats were purchased from the Animal Experiment Center of Suzhou University (Suzhou, China). Animal studies were performed with the approved protocol (NO. 2020012) by the Ethics Committee for Laboratory Animal Care of Animal studies of the Suzhou Hospital Affiliated to Nanjing University of Traditional Chinese Medicine (Suzhou, China). All rats were housed in a specific pathogen-free animal room under standard conditions with temperature (22–25 °C) with a 12-h light-dark cycle and had free access to standard laboratory food and water. All the experiments were performed in accordance with the Guide for the Care and Use of Laboratory Animals.

2.2. Animal experiments

8-week-old SD male rats were used for this study randomly. The rats were anesthetized by sodium pentobarbital (50 mg/kg, Sigma, USA) with intraperitoneal injection and underwent UUO of the left kidney using an established procedure [8]. All efforts were made to minimize animal suffering during and following surgery. The rats were randomly divided into three groups (n = 10): Sham group, UUO group, and UUO + Baicalein group respectively. Both sham and UUO group plus vehicle, UUO + Baicalein group plus 100 mg/kg Baicalein (cat #: 408240, Aladdin Shanghai, China) per day. The dosage of Baicalein was determined by a previous study based on the experiments of our laboratory [9]. Baicalein was dissolved in 0.1% dimethyl sulfoxide (DMSO) (Sigma-Aldrich, Dorset, UK), and the rats were given Baicalein daily for 14 days by oral gavage and operated by UUO surgery on the 15th day. The vehicle-treated Sham and UUO rats were administered with PBS in DMSO (10 mL/kg per day) for 14 days [10]. After 14 days of UUO surgery, rats were transferred into metabolic cages to collect urine for 24 h. After 15 days of UUO surgery, rats were anesthetized with secobarbital, blood samples were collected via retro-orbital puncture, and serum samples were separated by centrifugation (3000g, 15 min). Subsequently, rats were sacrificed by CO2 asphyxiation in the specific device and were performed by laparotomy to harvest left kidney tissue for weighing. The weight of the left kidney was normalized to the final body weight to calculate the left kidney mass index. The left kidneys were split into halves following the coronal plane. One-half was kept in 10% formalin for histopathological inspection. The other half was for further experiments.

2.3. Cell cultures

Renal podocyte MPC-5 cells were from the cell center of Beijing Union (Beijing, China) and cultured in complete RPMI1640 (GIBCO, USA) medium containing 10% fetal bovine serum and γ-interferon (10 U/mL) in 5% CO_2, 37 °C incubator for differentiation. 0.1 mg/mL of type I collagen (Manassas, VA) was placed on the bottom of culture plates to promote adherence before cell culture. The culture medium of MPC-5 cells without γ-interferon was used for culturing 10th to 14th days for differentiation. The extension of the foot process to the periphery indicated the beginning of mature differentiation. MPC-5 cells were treated with 0.0, 10^{-4}, 10^{-3}, 10^{-2}, 10^{-1},1.0 μM Erastin (cat #: E424821, Aladdin Shanghai, China) and 0.0, 0.1, 0.3, 1.0, 3.0 μM Baicalein, respectively. 0.1 μM Erastin combined with 0.1, 0.3, and 1.0 μM Baicalein were selected for further experiments. Baicalein was dissolved in 0.1% DMSO and added to cell culture for 24 h incubation. The survival rate of cultured cells was detected by Cell Counting Kit-8 (CCK-8) (Beyotime, Beijing, China) following the instructions. The culture medium and cell samples of MPC-5 cells were collected for further experiments respectively.

2.4. Renal function assay

Urinary albumin excretion was assessed by Urine protein Quantification Kit (Jiancheng Bioengineering Institute, Nanjing, China) with the CCB method. Serum creatinine (Scr) and blood urea nitrogen (BUN) levels were measured by Auto Biochemical Colorimetry Assays (Beckman AU5800, USA).

2.5. Renal morphology analysis

Hematoxylin and Eosin (HE) staining was performed according to the manufacturer's instructions. The renal tissue was isolated, fixed in 4% formaldehyde overnight, and embedded in paraffin. Renal interstitial lesions were characterized by the degree of changes in the glomerulus and tubules. At least 10 randomly chosen non-overlapping fields of view at a magnification of × 100 were observed and recorded for each slide. Renal interstitial lesions were graded on a scale from 0 to 4: 0, normal; 1, changes <25% of the cortex; 2, changes between 25 and 50% of the cortex; 3, changes between 50 and 75% of the cortex; and 4, changes >75% of the cortex. The total area occupied by fibrotic lesions was calculated for arbitrarily chosen fields of view and expressed as the percentage of fibrotic area relative to the entire image.

2.6. Perl's staining

Part of the renal tissue was fixed in 4% paraformaldehyde and then embedded in paraffin for slide preparation. For Perl's staining, the tissues were incubated in fresh Perl's solution (1:1, 5% potassium ferrocyanide, and 5% HCl) for 1 h, and washed with phosphate-buffered saline (PBS) for 3 times. A second incubation was performed in 0.5% diamine benzidine tetrahydrochloride. After rinsing twice, the slides were observed under light microscopy. The positive cells were quantified from random fields view at a magnification of × 200 of each tissue slide and analyzed by Image-Pro Plus 6.0 (Media Cybemetics, USA).

2.7. Masson staining

Tissue samples of kidney were fixed in 4% paraformaldehyde (PFA) and embedded in paraffin. Sections were cut at 5 μm, mounted on microscope slides and Masson Trichrome Staining was performed. After deparaffinization of slides, Bouin's Solution was applied for 15 min at 56 °C; the slides were washed to remove yellow color and after Hematoxylin staining for 5–10 min and washing with distilled water. Dissolve in acid ponceau for 5–10 min. Soak for a while with 2% ice acetic acid in water. Dissolve in 1% Phosphomolybdic acid aqueous solution for 3–5 min. Stain directly with aniline blue or light green solution for 5 min. Soak for a while with 0.2% ice acetic acid in water. Dehydrate in 95% ethyl alcohol for several times, followed by anhydrous alcohol. Hyalinise by dimethylbenzene and sealed by neutral balsam.

2.8. Iron assay

10 mg renal tissues of each group were cut and washed with cold PBS and then homogenized by vibrating immediately. For MPC5 cells, the collected cells were homogenized by ultrasonic. The relative iron concentrations in renal tissues and MPC5 cell lysates were assessed by Iron Assay Kit (Jiancheng Bioengineering Institute, Nanjing, China) following the manufacturer's instructions.

2.9. Measurement of the oxidative stress levels

A portion of the renal tissues was homogenized in saline solution for the analysis of ROS, malondialdehyde (MDA), and glutathione (GSH) levels. To assess the degree of lipid peroxidation, ROS, GSH (Jiancheng Bioengineering Institute, Nanjing, China), and MDA (Kaiji Bioengineering Institute, Nanjing, China) levels were measured by commercial assay kit according to the manufacturer's instructions. Oxidative stress in MPC-5 cells was determined by using the ROS Detection Kit (Jiancheng Bioengineering Institute, Nanjing, China). The intracellular ROS levels were determined by the intensity of DCFH-DA fluorescence. The relative intensity of fluorescence was quantified by Fluorescence Spectrophotometer (Synergy H4, Agilent, USA) at 488 nm excitation and 525 nm emission.

2.10. Western blot analysis

Tissues or cells were treated by RIPA lysis buffer (Solarbio, Beijing, China) and then homogenized on ice by Polytron Homogenizer (Königswinter, Germany). Protein concentrations were determined by BCA Protein Assay Kit (Thermo Fisher Scientific, Beijing, China). The target proteins were transferred from the SDS-PAGE gel to the PVDF membrane (Millipore, USA). After being blocked with 5% BSA in tris-buffered saline Tween-20 (TBST), the membrane was incubated with the primary antibodies overnight at 4 °C. Subsequently, the membranes were incubated with the secondary antibody (Beyotime Biotechnology, Shanghai, China) and conjugated to horseradish peroxidase for 1 h. The blots were visualized with ECL-Plus reagent (Santa Cruz, USA) and analyzed by Image-Pro Plus 6.0 (Media Cybemetics, USA). GAPDH was used as the loading control. The primary antibody was diluted in the primary antibody dilution buffer (Beyotime Biotechnology, Shanghai, China) according to the instructions. The information of primary antibodies used in experiments was as follows: glyceraldehyde-3-phosphate dehydrogenase (GAPDH) (cat #: ab8245, RRID:AB_2107448, Abcam, Cambridge, USA), TGF-β1 (cat #: ab215715, RRID:AB_2893156, Abcam, Cambridge, USA), Smad3 (cat #: ab40854, RRID:AB_777979, Abcam, Cambridge, USA), α-SMA (cat #: AF1032, RRID:AB_2835329, Affinity Bioscience, China), GPX4 (cat #: ab125066, RRID: AB_10973901, Abcam, Cambridge, USA), FTH (cat #: ab183781, RRID:AB_2940987, Abcam, Cambridge, USA), SLC7A11 (cat #: GTX89082, RRID:AB_10721569, Gene Tex, South California, USA).

2.11 Statistical analysis

The Experimental data are presented as the mean ± SEM. Statistical analysis was performed by GraphPad Prism (GraphPad Software, San Diego, CA, USA, RRID:SCR_002798). The comparison of two groups was analyzed by using Student's t-tests and the comparison of multiple groups was analyzed by analysis of variance between groups (ANOVA). The value of P less than 0.05 was considered to be a statistically significant difference.

(*P < 0.05, **P < 0.005, ***P < 0.001, $^{\#}$P < 0.05, $^{\#\#}$P < 0.005, $^{\#\#\#}$P < 0.001).

3. Results

3.1. Effects of Baicalein on kidney-related index and histological alteration in the UUO-induced animal model

Baicalein is a trihydroxyflavone with hydroxy groups at positions C-5, -6, and -7 (Fig. 1A). After 15 days of UUO surgery, the entire left kidney was dissected for weighing. It showed that the kidney weight index (the ratio of obstructed kidney weight to body weight) was almost 5 times more in the UUO group than that of the Sham group; however, Baicalein treatment attenuated the kidney weight index of the UUO group (Fig. 1B). Furthermore, the changes of 24h-urinary albumin excretion (nearly 2.5 times more), serum creatinine (32% higher), and BUN levels (nearly 1.8 times more) were significant in the UUO group than those in the Sham group; however, Baicalein treatment significantly reduced 24h-urinary albumin excretion, serum creatinine, and BUN levels (Fig. 1C–E). Histological examination of renal tissues by HE staining showed that the glomerular and tubular structures were intact in the sham group (Fig. 1F–I), however, glomerular capillaries dilated, and interstitial spaces become larger full of the infiltration of inflammatory cells and perivascular exudates in the UUO surgery group (Fig. 1G–J). Importantly, Baicalein treatment improved the morphological changes of renal tissue induced by UUO (Fig. 1H–K). Kidney tubular injury score showed there was almost 3.1 times changes in the

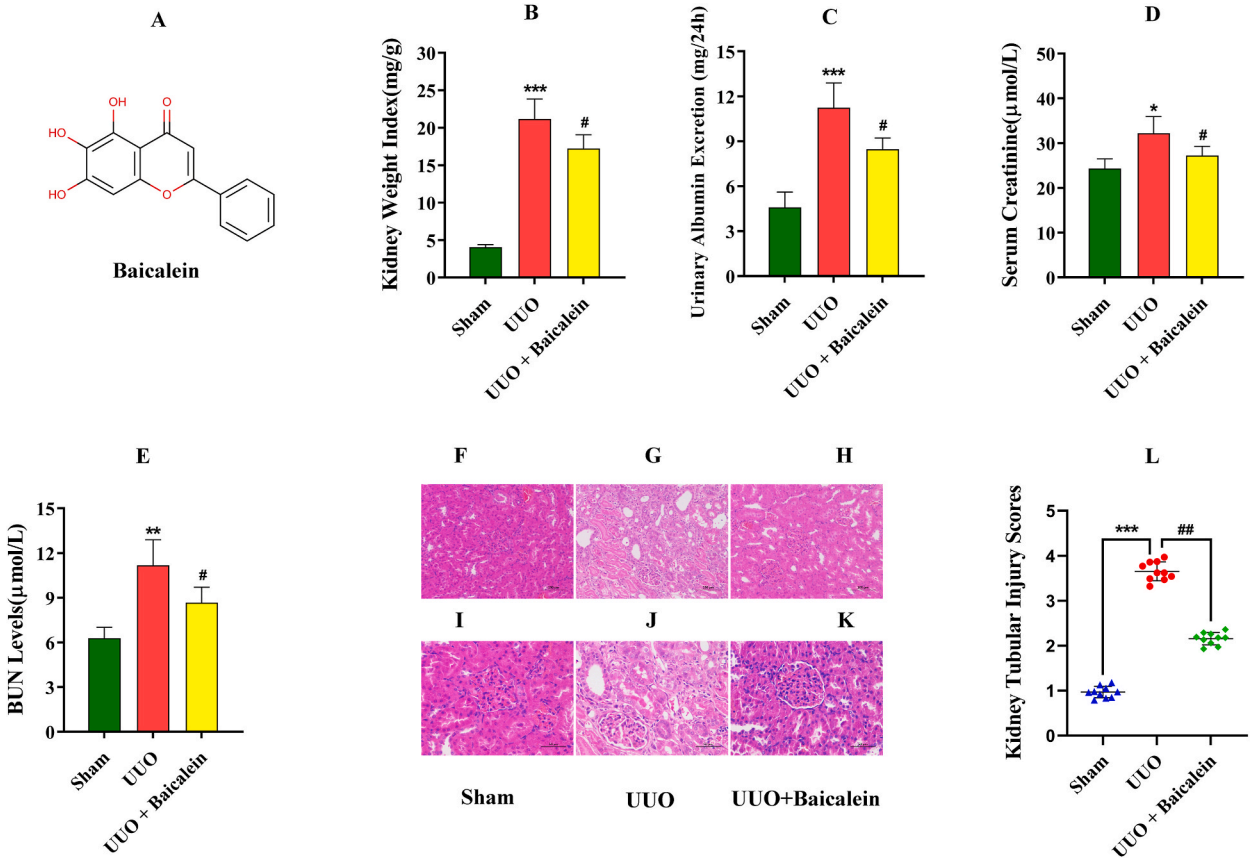

Fig. 1. Effects of Baicalein on kidney-related index and histological alteration in the UUO-induced animal model. (A) Chemical structure of baicalein. (B) Kidney weight index in rats (n = 10, ***P < 0.001 vs Sham group; #P < 0.05 vs UUO group). (C, D, and E) Measurement of 24h-urinary albumin excretion, serum creatinine, and BUN levels in the serum of rats (n = 10, ***P < 0.001 , *P < 0.05 and **P < 0.01 vs Sham group; #P < 0.05 vs UUO group). (F, G, and H) HE staining of renal tissue, groups of Sham, UUO, and UUO + Baicalein respectively (Scale bar = 200 μm). (I, J, and K) HE staining of renal tissue, groups of Sham, UUO, and UUO + Baicalein respectively (Scale bar = 100 μm). (L) Measurement of tubular injury scores based on HE staining (n = 5, ***P < 0.001 vs Sham group; #P < 0.05 vs UUO group). All the data are presented as mean ± SEM.

UUO group than that of the Sham group; while Baicalein treatment reduced 43% injury of kidney tube (Fig. 1L).

3.2. Effect of Baicalein on ferroptosis-related index in the UUO animal model

Perls' staining is a regular method for staining non-haem iron in normoblasts, macrophages, and other cells containing particulate iron (Fig. 2A–C). Masson staining is one of the most classical methods of connective tissue staining for showing fibers in tissues, especially for collagen fibers (Fig. 2D–F). There are almost 18 time more iron-positive cells in the UUO group than those of the Sham group, while Baicalein treatment reduced nearly 40% the number of iron-positive cells compared with those of the UUO group (Fig. 2G). The iron concentration increased 2.4 times more in the UUO group than those of the Sham group, while Baicalein treatment reduced nearly 27% compared with that of the UUO group (Fig. 2H). Similarly, the result of Masson staining had the same tendency as those of Perls' staining (Fig. 2D–F). Furthermore, the changes of ROS level (nearly 5.4 times) and MDA level (nearly 4.7 times) were significant in the UUO group than those of the Sham group respectively, while Baicalein reduced the levels of ROS (34%) and MDA (39%) compared with those of the UUO group (Fig. 2I and J). Other ferroptosis biomarkers such as GSH and SOD exhibited lower levels in the UUO group than those of the Sham group, however, Baicalein treatment significantly improved the reduction of the GSH and SOD levels in UUO group (Fig. 2K and L).

3.3. Effect of Baicalein on the proteins of fibrosis-related and ferroptosis-related in UUO animal model

The SLC7A11-GSH-GPX4 axis is well-known as an important marker in regulating ferroptosis. The main function of GPX4 is converting GSH to oxidized glutathione (GSSG) and reducing cytotoxic lipid peroxides to their corresponding alcohols [11], while inhibition of GPX4 will result in the accumulation of GSH and lipid peroxidation that will trigger ferroptosis of cells [12]. Ferritin heavy chain (FTH) is mainly responsible for the assembly of stable ferritin complexes and the formation of iron reserves, which has the property of ferroxidase to prevent the iron-mediated production of ROS [13]. In our study, it was found that profibrotic factors such as

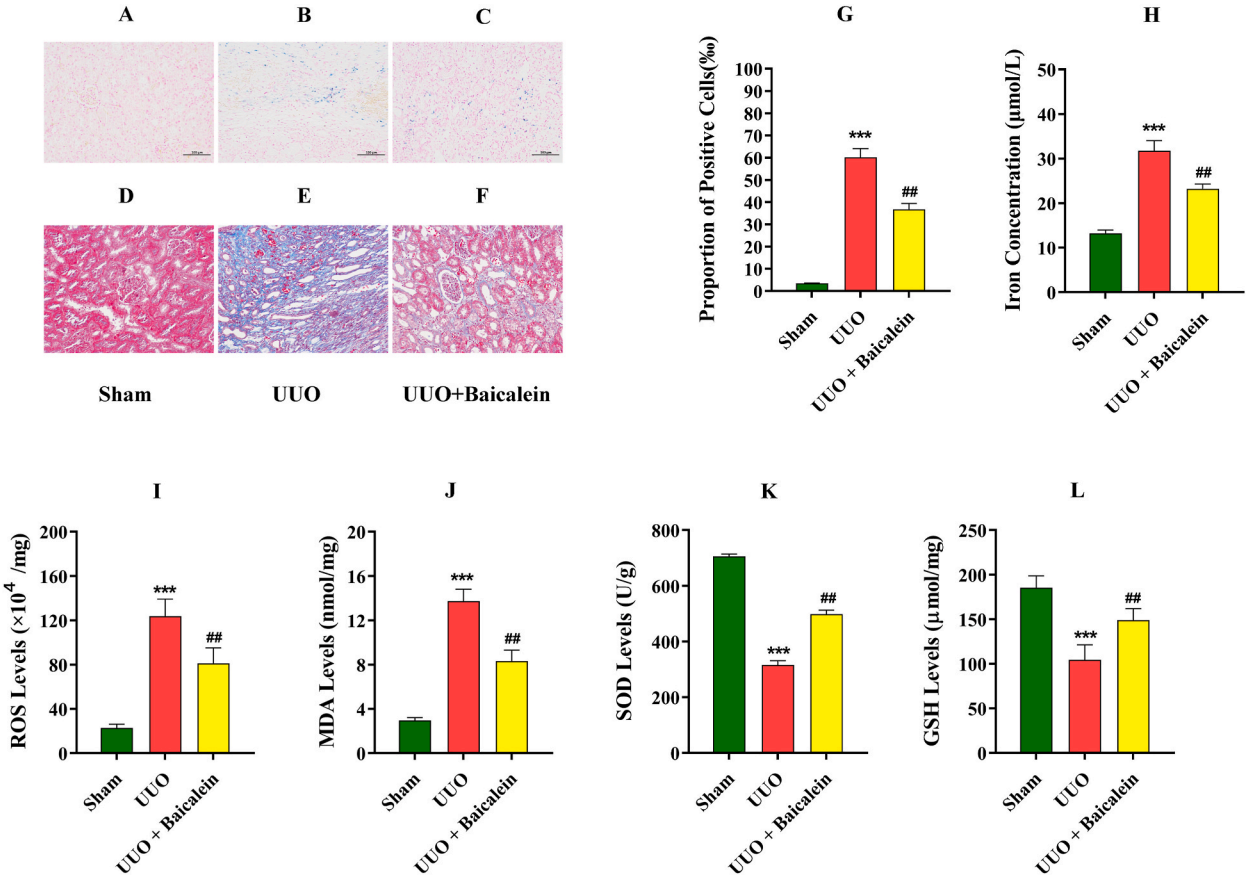

Fig. 2. Effect of Baicalein on ferroptosis-related index in the UUO animal model. (A, B and C) Perl's staining of kidney tissues (Scale bar = 100 μm). (D, E and F) Masson staining of kidney tissues (Scale bar = 100 μm). (G and H) Iron-positive cells counted on Perl's staining and iron concentration detected in the kidney (n = 5, ***$P < 0.001$ vs Sham group; ##$P < 0.01$ vs UUO group). (I, J, K, and L) ROS, MDA, SOD, and GSH levels were measured in the kidney of different groups (n = 10, ***$P < 0.001$ vs Sham group; ##$P < 0.01$ vs UUO group). All the data are presented as the mean ± SEM.

TGF-β1 (1.56 times), Smad3 (2.9 times), and α-SMA (2.2 times) were upregulated greatly in the UUO group compared with those of the Sham group, however, Baicalein treatment reduced the expression of TGF-β1 (44%), Smad3 (94%), and α-SMA (23%) compared with those of the UUO group respectively (Fig. 3A–D, Supplementary Fig. 1). It showed that the UUO surgery increased the phosphorylation level of Smad3 (3 times) significantly than that of the Sham group, while Baicalein treatment reduced the phosphorylation level of Smad3 (55%) compared with that of the UUO group (Fig. 3E and F, Supplementary Fig. 1). For ferroptosis, SLC7A11 (46%), GPX4 (49%), and FTH (51%) were downregulated greatly in the UUO group compared with those of the Sham group, while Baicalein treated group promoted their expression levels significantly than those of the UUO group (Fig. 3G–J, Supplementary Fig. 1).

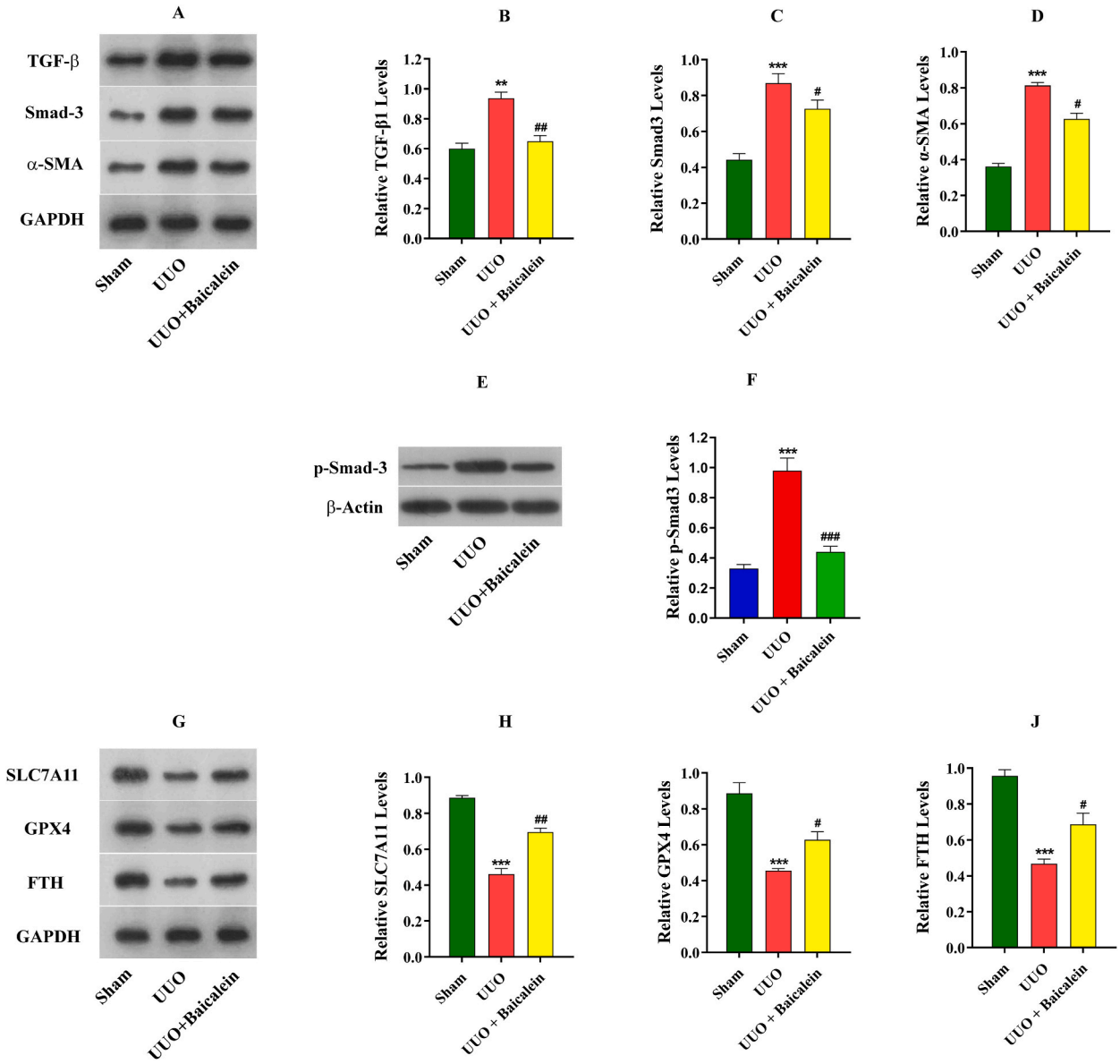

Fig. 3. Effect of Baicalein on the proteins of fibrosis-related and ferroptosis-related in UUO animal model. (A) Western blot gel graph of TGF-β1, Smad3, and α-SMA in renal tissues of rats. (B, C, and D) Semi-quantitative analysis of the expression of TGF-β1, Smad3, and α-SMA in the different groups (n = 5, $^{**}P < 0.01$ and $^{***}P < 0.001$ vs Sham group; $\#\#P < 0.01$ and $\#P < 0.05$ vs UUO group). (E) Western blot gel graph of Smad3 phosphorylation in renal tissues of rats. (F) Semi-quantitative analysis of the expression of Smad3 phosphorylation in the different groups (n = 5, $^{***}P < 0.001$ vs Sham group; $\#\#\#P < 0.001$ vs UUO group). (G) Western blot gel graph of SLC7A11, GPX4, and FTH in renal tissues of rats. (H, I, and J) Semi-quantitative analysis of the expression of SLC7A11, GPX4, and FTH in the different groups. (n = 5, $^{***}P < 0.001$ vs Sham group; $\#\#P < 0.01$ and $\#P < 0.05$ vs UUO group). All the data are presented as the mean ± SEM.

3.4. Construct the ferroptosis model induced by Erastin in MPC-5 cells

Erastin is one of potent ferroptosis inducers by inhibiting voltage-dependent anion-selective channels (VDAC2 and VDAC3) directly (Fig. 4A). To construct the ferroptosis model in MPC5 cells, we set 5 different concentration gradients (10-fold intervals) of Erastin. MPC5 cells were treated with (0, 10^{-4}, 10^{-3}, 10^{-2}, 0.1, and 1 μM) of Erastin for 24 h, we found that 0.1 μM Erastin inhibited 20%–30% viability of MPC5 cells by CCK-8 assay (Fig. 4B). So, 0.1 μM Erastin was selected for further experiments. It was found that intracellular ROS levels (1.88 times) and Iron concentration (26%) increased significantly in the Erastin-induced group than those of the control group (Fig. 4C and D). To measure the cytotoxic effects of Baicalein, we detected the cell viability of the MPC-5 cells under Baicalein treatment with different concentration gradients (3-fold intervals). It showed that Baicalein with the range of 0.1–1.0 μm did not affect the viability of MPC-5 cells after 24 h of treatment, however, the cell survival rate was significantly lower under 3.0 μm of Baicalein (Fig. 4E). To find out the optimal combination of the induction by Erastin and the treatment by Baicalein, we treated MPC-5 cells with 0.1, 0.3, and 1 μM of Baicalein under 0.1 μM Erastin-induced. It was found that 1 μM of Baicalein was the optimal concentration for ferroptosis inhibition (Fig. 4F). In further measurement, the intracellular ROS levels (1.97 times) and Iron concentration (1.39 times) were significantly higher in the Erastin-induced group than those of the control group, while both of them reduced nearly 20% in Baicalein treated (1 μM) group compared with those of the Erastin-induced group (Fig. 4G and H).

3.5. Effect of Baicalein on the proteins of fibrosis-related and ferroptosis-related in the Erastin-induced MPC-5 cells

In the Erastin-induced MPC-5 cells, TGF-β1, Smad3, and α-SMA were used as the biomarkers to detect fibrosis, and SLC7A11, GPX4, and FTH were used to detect ferroptosis respectively. The results of Western blot showed that MPC-5 cells induced by Erastin significantly increased the expression of TGF-β1 (1.63 times), Smad3 (1.93 times), and α-SMA (1.85 times) compared with those of the control group, while Baicalein treatment reduced their expression levels (33%, 46%, and 38% respectively) greatly against those of the Erastin-induced group (Fig. 5A–D, Supplementary Fig. 2). In terms of Ferroptosis, Erastin-induced MPC-5 cells presented lower expression levels of SLC7A11 (34%), GPX4 (44%), and FTH (61%), however, Baicalein treatment increased their expression (32%,

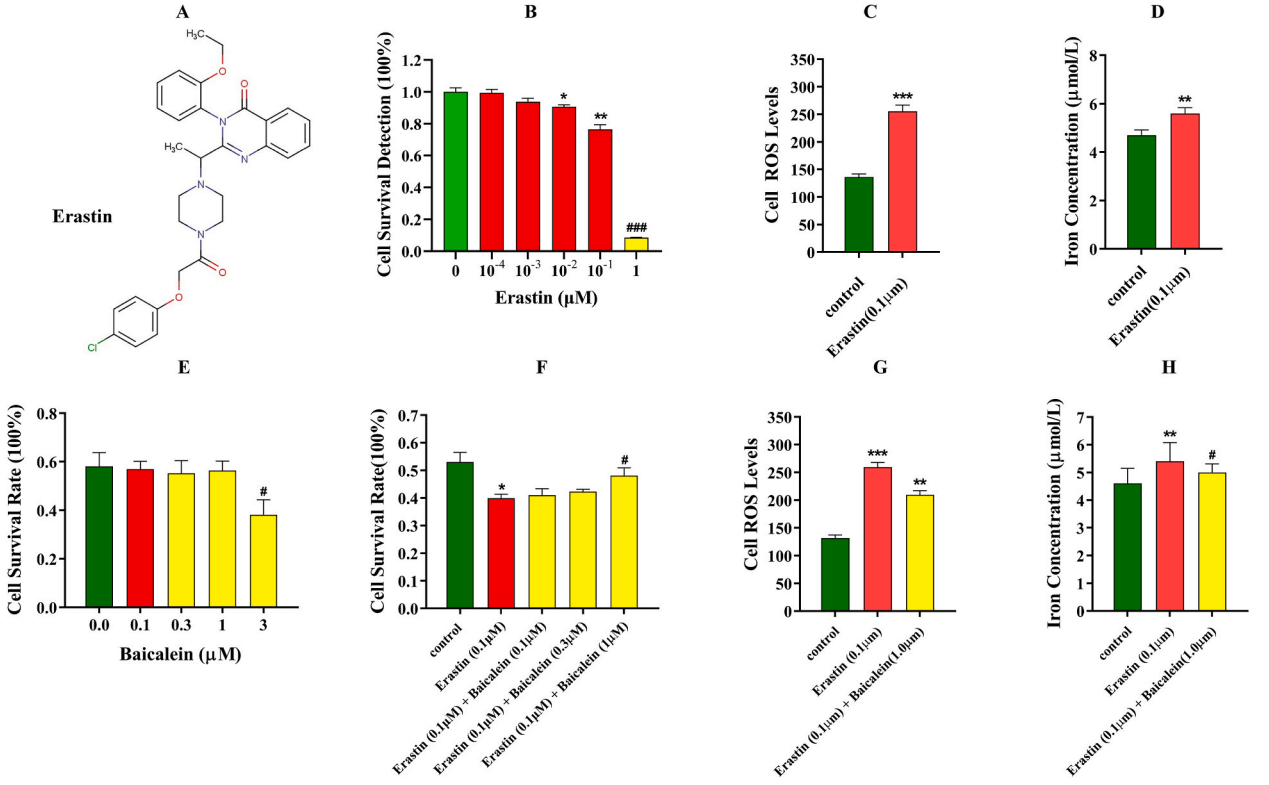

Fig. 4. Construct the ferroptosis model induced by Erastin in MPC-5 cells. (A) Chemical structure of baicalein. (B) Viability of MPC-5 cells induced by Erastin (n = 6, $*P < 0.05$ and $**P < 0.01$ vs control group respectively; $\#\#\#P < 0.001$ vs 10^{-1} mM Erastin group). (C and D) ROS levels and Iron concentration under the induction of 0.1 μM Erastin (n = 6, $***P < 0.001$ and $**P < 0.01$ vs control group). (E) Viability of MPC-5 cells under different concentrations of Baicalein treatment. (n = 6, $\#P < 0.05$ vs control group). (F) Viability of Erastin-induced MPC-5 cells under 0.1, 0.3, and 1 μM treatment of Baicalein (n = 6, $*P < 0.05$ vs control group; $\#P < 0.05$ vs 10^{-1} μM Erastin group). (G and H) ROS levels and Iron concentration in 0.1M Erastin-induced MPC-5 cells under treatment of 1.0 μM (n = 6, $**P < 0.01$ vs control group respectively; $\#\#P < 0.01$ and $\#P < 0.05$ vs 10^{-1} μM Erastin group respectively). All the data are presented as the mean ± SEM.

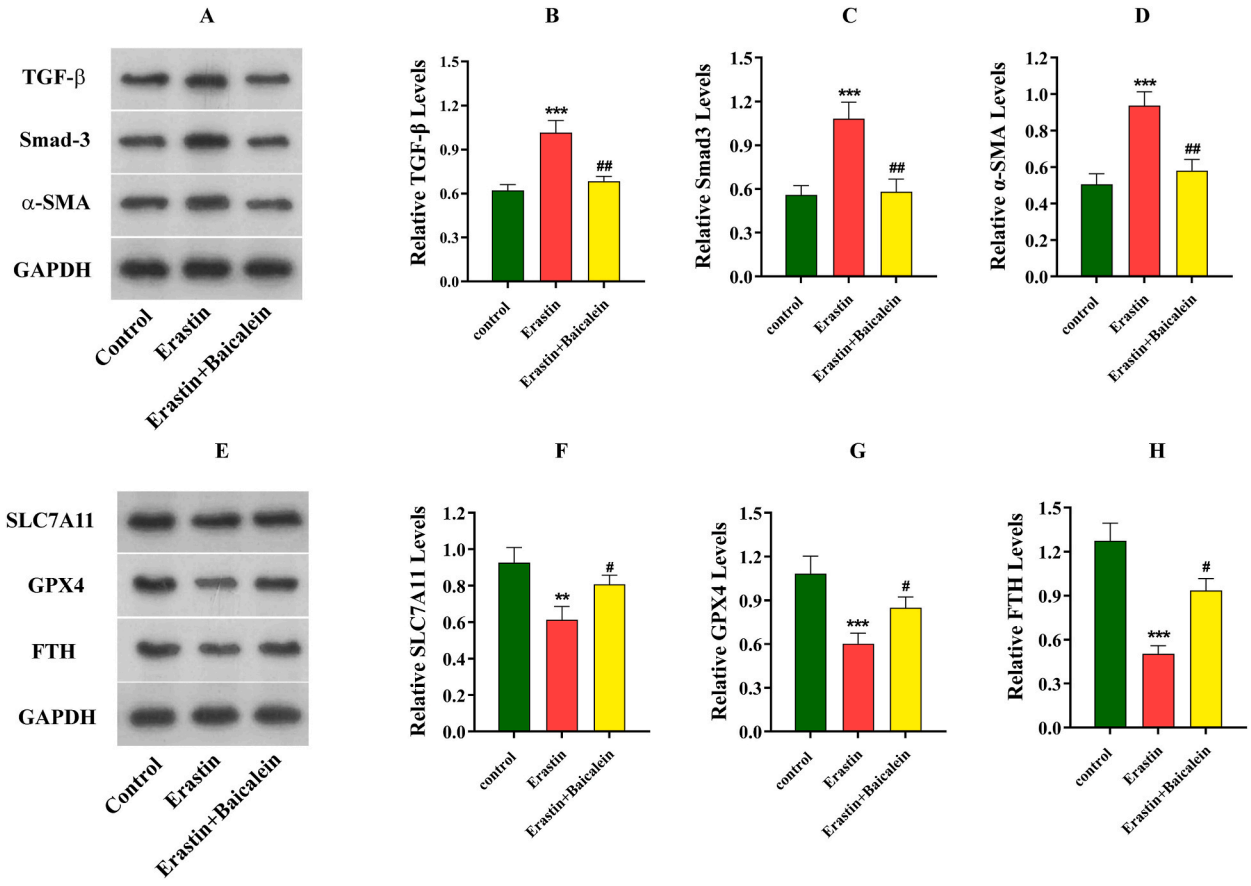

Fig. 5. Effect of Baicalein on the proteins of fibrosis-related and ferroptosis-related in the Erastin-induced MPC-5 cells. (A) Western blot gel graph of TGF-β1, Smad3, and α-SMA in MPC-5 cells. (B, C and D) Semi-quantitative analysis of TGF-β1, Smad3, and α-SMA in the different groups of MPC-5 cells (n = 5, $***P < 0.001$ vs control group; $\#\#P < 0.01$ vs Erastin group). (E) Western blot gel graph of SLC7A11, GPX4, and FTH in MPC-5 cells; (F, G, and H) Semi-quantitative analysis of SLC7A11, GPX4, and FTH in the different groups of MPC-5 cells. (n = 5, $**P < 0.01$ and $***P < 0.001$ vs control group; $\#P < 0.05$ vs Erastin group). All of the data are presented as the mean ± SEM.

41%, 86% respectively) greatly than those of the Erastin-induced group (Fig. 5E–H, Supplementary Fig. 2

4. Discussion

RIF and tubular atrophy are closed related to the decline in renal function in chronic kidney diseases (CKD), which affects more than 10% population of the world [14]. The underlying mechanism of RIF is so complicated that including the events such as activation of mesangial and fibroblast, infiltration of monocyte/macrophage and T-cell, transition of tubular epithelial to mesenchymal and cell apoptosis [15,16]. It is well known that podocytes had a very limited potentiality for regeneration. Loss of podocytes in glomeruli is considered an irreversible process in the pathology of CKD [17,18]. In our study, we made a rat model by UUO method, which is an ideal pathological model to be used to study the RIF *in vivo* (Figs. 1 and 2), and used Erastin-induced MPC-5 cells to investigate the role of Baicalein in the process of RIF *in vitro* (Figs. 4 and 5). The pro-fibrotic factors TGF-β1, Smad3, and α-SMA were selected to verify the degree of RIF improved by Baicalein both in UUO rats' model *in vivo* and Erastin-induced MPC-5 cells *in vitro* (Figs. 3 and 5).

It was found that ferroptosis played an important role in acute kidney injury, renal cancer, and other kidney-related diseases, however, its underlying mechanism has not been fully elucidated [18,19]. Cystine/glutamate antiporter (System Xc) is an important intracellular antioxidant system, including two subunits termed SLC7A11 and SLC3A2L, which can take up cystine and excrete glutamate [20]. Interestingly, the inhibition of System Xc triggers cell ferroptosis [21,22], the increase of SLC7A11 can significantly inhibit ferroptosis [20]. Cystine is reduced to cysteine after being ingested by System Xc and participates in the synthesis of GSH [23,24]. Furthermore, the inhibition of cystine transfer by Erastin reduced the source of cysteine, which is an essential component of GSH that is regulated by GPX4 in ferroptosis [25,26]. In addition, when GPX4 is knocked out in the kidney, acute renal failure can be inhibited by the ferroptosis inhibitor Ferrostatin-1 [27,28]. Ferritin is composed of two subunits of a heavy chain (FTH) and light chain (FTL) to form a spherical shell cavity structure, which stores high concentrations of iron, thereby preventing exposure to substrates that generate active oxygen [29]. Inhibition of the expression of iron response element-binding protein 2 (IREB2), a major transcription

factor for iron metabolism, significantly increased the expression of FTL and FTH1, thereby suppressing induced ferroptosis [30,31]. It was reported that the expression of FTH1 and FTL was significantly increased in ferroptosis-insensitive cells compared with ferroptosis-sensitive cells, however, autophagy can promote the degradation of ferritins FTL and FTH1 respectively, thereby increasing the iron content in cells and leading to ferroptosis [32,33]. From the above-mentioned, SLC7A11, GPX4, and FTH1 play an important role in regulating ferroptosis. In our study, we found that Baicalein inhibited ferroptosis-related factors such as SLC7A11, GPX4, and FTH1 both in UUO animal model and Erastin-reduced MPC-5 cells (Figs. 3 and 5). It demonstrated that Baicalein had a potential therapeutic effect on renal disease treatment.

Baicalein, a nature flavonoid product, has been widely used as a treatment for microbial infection diseases in East Asian countries for a long time. Currently, several studies reported that Baicalein was a potential anti-fibrotic agent, which prevents the progression of liver fibrosis induced by carbon tetrachloride, alleviates RIF by reducing ECM production, and repressing TGF-β1 expression in the UUO model [34–36]. Normally, the RIF are usually quiescent in kidney, however, they are activated by TGF-β1 and subsequently express fibroblast specific protein-1 (FSP-1), a-SMA, or vimentin to transform into myofibroblasts phenotypically after chronic injury. Baicalein was reported to block the PI3k/Akt signaling induced by TGF-β1 to activate mitochondrial apoptosis in myofibroblasts, which might be one of the mechanisms of RIF inhibition [4]. For ferroptosis, Baicalein presented remarkable anti-ferroptosis activity in the reduction of iron ion production, glutathione depletion, and lipid peroxidation [37]. For another, Baicalein can suppress Erastian-induced degradation of GPX4, which is a phospholipid hydroperoxidase that protects cells against membrane lipid peroxidation [38]. Thus, together with previous studies, we hypothesized that maybe Baicalein attenuated RIF by inhibiting the ferroptosis of podocytes that is one of the important cell types in the renal interstitial. Interestingly, our data supported the assumption that Baicalein was able to improve RIF both in the UUO-induced animal model and Erastin-induced MPC-5 cells by inhibiting TGF-β1, a-SMA and Smad-2 expression (Figs. 3 and 5), which suggested that Baicalein had played a role in renal protection and antifibrotic activity. Furthermore, Baicalein was also able to inhibit ferroptosis both in a rat UUO model and Erastin-induced MPC-5 cells via reducing the expression of SLC7A11, GPX4, and FTH (Figs. 3 and 5), those of which are key biomarkers in ferroptosis. HE and Perls' staining also supported the protective effect of Baicalein on preventing cell morphological changes and reducing iron deposited in renal cells of the rats UUO model respectively (Figs. 1 and 2). In addition, 1.0 μM Baicalein significantly attenuated fibrosis in the 0.1 μM Erastin-induced MPC-5 cells (Fig. 5). Therefore, based on above mentioned, our hypothesis on the relationship between RIF and ferroptosis mediated by Baicalein has been confirmed.

However, the findings of this study have to be seen in light of some limitations.

The first is that only one RIF animal model was used in the study. It is necessary to apply other RIF animal models to investigate the effect of Baicalein. The second limitation concerns that RIF is a chronic irreversible and complicated pathological change that a variety of different kidney cells are involved. Consequently, the investigation on the renal podocyte (MPC-5 cells) is not enough to provide the overall picture on fighting against RIF by the action of Baicalein through triggering cell ferroptosis. Therefore, we should conduct research on other renal cells to clarify the action mechanism of Baicalein.

5. Conclusion

In summary, (1) our study demonstrated that ferroptosis occurred in the kidney of the UUO-induced animal model. (2) Baicalein was able to improve UUO-induced RIF by inhibiting ferroptosis. (3) we have constructed an Erastin-induced ferroptosis model in MPC-5 cells for measuring the antifibrotic and anti-ferroptosis effects of Baicalein successfully. (4) Baicalein was able to attenuate RIF in the Erastin-induced MPC-5 cells by inhibiting ferroptosis. In conclusion, our findings provide a novel mechanism on the antifibrotic effect of Baicalein and a new perspective in the treatment of RIF in clinical settings. In the future, studies of other animals even clinical trials and investigations into the roles of other signaling pathways are necessary.

Funding sources

This research was supported by the National Natural Science Foundation, China (82074368). Top Scientific Research Project of "Six and One Project" for High-level Health Talents in Jiangsu Province (LGY2020046). The fifth ninth Batch of Suzhou Gusu Top Key Health Talents Project (GSWS2019063, GSWS2022107) and the Key Technology Project of Suzhou Science and Technology Plan (Medical and Health Technology Innovation) (SKY2021058).

Ethical approval

The animal experiments involved in the study were conducted under the permission of the Ethics Committee for Laboratory Animal Care of Animal studies were performed with the approved protocol by the Suzhou Hospital Affiliated to Nanjing University of Traditional Chinese Medicine. (Animal Ethics Regulations and Guidelines of the People's Republic of China) (License No. 2020012)

Data availability statement

The data that support the findings of this study are available from the corresponding author upon reasonable request.

CRediT authorship contribution statement

Guo-qiang Liang: Writing – original draft, Methodology, Investigation. **Wei Mu:** Writing – original draft, Validation, Investigation, Formal analysis. **Chun-bo Jiang:** Supervision, Funding acquisition, Conceptualization.

Declaration of competing interest

The authors declare that they have no known competing financial interests or personal relationships that could have appeared to influence the work reported in this paper.

Appendix A. Supplementary data

Supplementary data to this article can be found online at https://doi.org/10.1016/j.heliyon.2024.e28954.

References

[1] M. Li, F. Jia, H. Zhou, J. Di, M. Yang, Elevated aerobic glycolysis in renal tubular epithelial cells influences the proliferation and differentiation of podocytes and promotes renal interstitial fibrosis, Eur. Rev. Med. Pharmacol. Sci. 22 (16) (2018) 5082–5090.
[2] F. Deng, I. Sharma, Y. Dai, M. Yang, Y.S. Kanwar, Myo-inositol oxygenase expression profile modulates pathogenic ferroptosis in the renal proximal tubule, J. Clin. Invest. 129 (11) (2019) 5033–5049.
[3] J.P. Friedmann Angeli, M. Schneider, B. Proneth, Y.Y. Tyurina, V.A. Tyurin, V.J. Hammond, N. Herbach, M. Aichler, A. Walch, E. Eggenhofer, D. Basavarajappa, O. Radmark, S. Kobayashi, T. Seibt, H. Beck, F. Neff, I. Esposito, R. Wanke, H. Forster, O. Yefremova, M. Heinrichmeyer, G.W. Bornkamm, E.K. Geissler, S. B. Thomas, B.R. Stockwell, V.B. O'Donnell, V.E. Kagan, J.A. Schick, M. Conrad, Inactivation of the ferroptosis regulator Gpx4 triggers acute renal failure in mice, Nat. Cell Biol. 16 (12) (2014) 1180–1191.
[4] Y.C. Hou, S.P. Lin, S.Y. Tsai, M.H. Ko, Y.C. Chang, P.D. Chao, Flavonoid pharmacokinetics and tissue distribution after repeated dosing of the roots of Scutellaria baicalensis in rats, Planta Med. 77 (5) (2011) 455–460.
[5] W. Wang, P.H. Zhou, C.G. Xu, X.J. Zhou, W. Hu, J. Zhang, Baicalein attenuates renal fibrosis by inhibiting inflammation via down-regulating NF-kappaB and MAPK signal pathways, J. Mol. Histol. 46 (3) (2015) 283–290.
[6] M. Yang, X. Li, H. Li, X. Zhang, X. Liu, Y. Song, Baicalein inhibits RLS3-induced ferroptosis in melanocytes, Biochem. Biophys. Res. Commun. 561 (2021) 65–72.
[7] Q. Li, Q.Q. Li, J.N. Jia, Q.Y. Sun, H.H. Zhou, W.L. Jin, X.Y. Mao, Baicalein exerts neuroprotective effects in FeCl(3)-induced posttraumatic epileptic seizures via suppressing ferroptosis, Front. Pharmacol. 10 (2019) 638.
[8] Z. Shi, Q. Wang, Y. Zhang, D. Jiang, Extracellular vesicles produced by bone marrow mesenchymal stem cells attenuate renal fibrosis, in part by inhibiting the RhoA/ROCK pathway, in a UUO rat model, Stem Cell Res. Ther. 11 (1) (2020) 253.
[9] P. Fu, Q. Yuan, Y. Sun, X. Wu, Z. Du, Z. Li, J. Yu, K. Lv, J. Hu, Baicalein ameliorates Epilepsy Symptoms in a Pilocarpine-induced rat model by regulation of IGF1R, Neurochem. Res. 45 (12) (2020) 3021–3033.
[10] K. Yang, B. Fan, Q. Zhao, Y. Ji, P. Liu, S. Gao, T. Ren, Y. Dou, M. Pei, H. Yang, Hirudin ameliorates renal interstitial fibrosis via regulating TGF-beta1/Smad and NF-kappaB signaling in UUO rat model, Evid Based Complement Alternat Med 2020 (2020) 7291075.
[11] L. Flohe, S. Toppo, L. Orian, The glutathione peroxidase family: Discoveries and mechanism, Free Radic. Biol. Med. 187 (2022) 113–122.
[12] F. Tian, Z.Y. Zhang, J. Sun, Y.C. Han, Expression of miR-207 in renal tissue of renal fibrosis rats and its correlation analysis with protein expression of TGF-beta1 and Smad3, Eur. Rev. Med. Pharmacol. Sci. 25 (2) (2021) 787–794.
[13] W. Hu, C. Zhou, Q. Jing, Y. Li, J. Yang, C. Yang, L. Wang, J. Hu, H. Li, H. Wang, C. Yuan, Y. Zhou, X. Ren, X. Tong, J. Du, Y. Wang, FTH promotes the proliferation and renders the HCC cells specifically resist to ferroptosis by maintaining iron homeostasis, Cancer Cell Int. 21 (1) (2021) 709.
[14] X. Li, S. Zhuang, Recent advances in renal interstitial fibrosis and tubular atrophy after kidney transplantation, Fibrogenesis Tissue Repair 7 (2014) 15.
[15] T.D. Hewitson, W.Y. Ho, C.S. Samuel, Antifibrotic properties of relaxin: in vivo mechanism of action in experimental renal tubulointerstitial fibrosis, Endocrinology 151 (10) (2010) 4938, 48.
[16] H.A. Chen, C.M. Chen, S.S. Guan, C.K. Chiang, C.T. Wu, S.H. Liu, The antifibrotic and anti- inflammatory effects of icariin on the kidney in a unilateral ureteral obstruction mouse model, Phytomedicine 59 (2019) 152917.
[17] B.D. Humphreys, Mechanisms of renal fibrosis, Annu. Rev. Physiol. 80 (2018) 309–326.
[18] I.S. Daehn, J.S. Duffield, The glomerular filtration barrier: a structural target for novel kidney therapies, Nat. Rev. Drug Discov. 20 (10) (2021) 770–788.
[19] L. Yang, Y. Liu, S. Zhou, Q. Feng, Y. Lu, D. Liu, Z. Liu, Novel insight into ferroptosis in kidney diseases, Am. J. Nephrol. (2023) 1.
[20] R. Bridges, V. Lutgen, D. Lobner, D.A. Baker, Thinking outside the cleft to understand synaptic activity: contribution of the cystine-glutamate antiporter (System xc-) to normal and pathological glutamatergic signaling, Pharmacol. Rev. 64 (3) (2012) 780–802.
[21] S.J. Dixon, K.M. Lemberg, M.R. Lamprecht, R. Skouta, E.M. Zaitsev, C.E. Gleason, D.N. Patel, A.J. Bauer, A.M. Cantley, W.S. Yang, B. Morrison 3rd, B. R. Stockwell, Ferroptosis: an iron- dependent form of nonapoptotic cell death, Cell 149 (5) (2012) 1060–1072.
[22] L.C. Chang, S.K. Chiang, S.E. Chen, Y.L. Yu, R.H. Chou, W.C. Chang, Heme oxygenase-1 mediates BAY 11-7085 induced ferroptosis, Cancer Lett. 416 (2018) 124–137.
[23] L. Chen, X. Li, L. Liu, B. Yu, Y. Xue, Y. Liu, Erastin sensitizes glioblastoma cells to temozolomide by restraining xCT and cystathionine-gamma-lyase function, Oncol. Rep. 33 (3) (2015) 1465–1474.
[24] F.J. Li, H.Z. Long, Z.W. Zhou, H.Y. Luo, S.G. Xu, L.C. Gao, System X(c) (-)/GSH/GPX4 axis: an important antioxidant system for the ferroptosis in drug-resistant solid tumor therapy, Front. Pharmacol. 13 (2022) 910292.
[25] P. Lei, S. Ayton, A.I. Bush, The essential elements of Alzheimer's disease, J. Biol. Chem. 296 (2021) 100105.
[26] S. Hao, J. Yu, W. He, Q. Huang, Y. Zhao, B. Liang, S. Zhang, Z. Wen, S. Dong, J. Rao, W. Liao, M. Shi, Cysteine Dioxygenase 1 mediates Erastin-induced ferroptosis in Human Gastric cancer cells, Neoplasia 19 (12) (2017) 1022–1032.
[27] J. Shao, Z. Bai, L. Zhang, F. Zhang, Ferrostatin-1 alleviates tissue and cell damage in diabetic retinopathy by improving the antioxidant capacity of the Xc (-)-GPX4 system, Cell Death Dis. 8 (1) (2022) 426.
[28] J. Shao, Z. Bai, L. Zhang, F. Zhang, Ferrostatin-1 alleviates tissue and cell damage in diabetic retinopathy by improving the antioxidant capacity of the Xc (-)-GPX4 system, Cell Death Dis. 8 (1) (2022) 426.
[29] L. Houben, H. Weissman, S.G. Wolf, B. Rybtchinski, A mechanism of ferritin crystallization revealed by cryo-STEM tomography, Nature 579 (7800) (2020) 540–543.
[30] E. Mishima, The E2F1-IREB2 axis regulates neuronal ferroptosis in cerebral ischemia, Hypertens. Res. 45 (6) (2022) 1085–1086.
[31] A.K. Hernandez-Gallardo, F. Missirlis, Loss of ferritin in developing wing cells: apoptosis and ferroptosis coincide, PLoS Genet. 16 (1) (2020) e1008503.

[32] J. Liu, Z. Ren, L. Yang, L. Zhu, Y. Li, C. Bie, H. Liu, Y. Ji, D. Chen, M. Zhu, W. Kuang, The NSUN5- FTH1/FTL pathway mediates ferroptosis in bone marrow-derived mesenchymal stem cells, Cell Death Dis. 8 (1) (2022) 99.
[33] W. Hou, Y. Xie, X. Song, X. Sun, M.T. Lotze, H.J. Zeh 3rd, R. Kang, D. Tang, Autophagy promotes ferroptosis by degradation of ferritin, Autophagy 12 (8) (2016) 1425–1428.
[34] E.K. Kong, S. Yu, J.E. Sanderson, K.B. Chen, Y. Huang, C.M. Yu, A novel anti-fibrotic agent, baicalein, for the treatment of myocardial fibrosis in spontaneously hypertensive rats, Eur. J. Pharmacol. 658 (2–3) (2011) 175–181.
[35] H. Sun, Q.M. Che, X. Zhao, X.P. Pu, Antifibrotic effects of chronic baicalein administration in a CCl4 liver fibrosis model in rats, Eur. J. Pharmacol. 631 (1–3) (2010) 53–60.
[36] W. Wang, P.H. Zhou, C.G. Xu, X.J. Zhou, W. Hu, J. Zhang, Baicalein ameliorates renal interstitial fibrosis by inducing myofibroblast apoptosis in vivo and in vitro, BJU Int. 118 (1) (2016) 145–152.
[37] Y. Xie, W. Hou, X. Song, Y. Yu, J. Huang, X. Sun, R. Kang, D. Tang, Ferroptosis: process and function, Cell Death Differ. 23 (3) (2016) 369–379.
[38] Y. Xie, X. Song, X. Sun, J. Huang, M. Zhong, M.T. Lotze, H.J.R. Zeh, R. Kang, D. Tang, Identification of baicalein as a ferroptosis inhibitor by natural product library screening, Biochem. Biophys. Res. Commun. 473 (4) (2016) 775–780.